Journal of Materials Chemistry A

Materials for energy and sustainability

www.rsc.org/MaterialsA

Volume 1 | Number 24 | 28 June 2013 | Pages 6971–7278

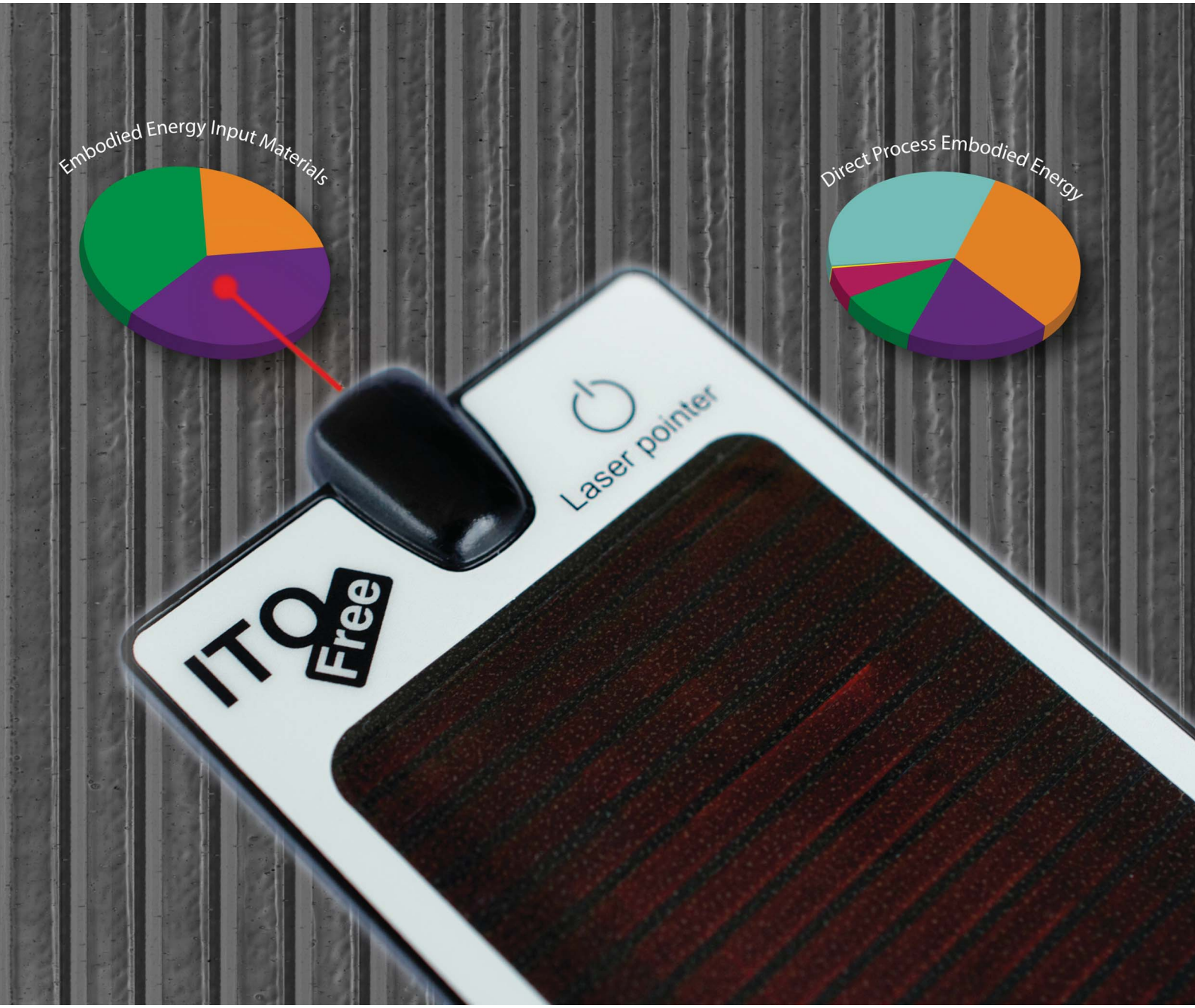

ISSN 2050-7488

RSC Publishing

PAPER

Frederik C. Krebs *et al.*

OPV for mobile applications: an evaluation of roll-to-roll processed indium and silver free polymer solar cells through analysis of life cycle, cost and layer quality using inline optical and functional inspection tools

2050-7488(2013)1:24;1-X

Journal of Materials Chemistry A

RSC Publishing

PAPER

View Article Online
View Journal | View Issue

Cite this: J. Mater. Chem. A, 2013, 1, 7037

OPV for mobile applications: an evaluation of roll-to-roll processed indium and silver free polymer solar cells through analysis of life cycle, cost and layer quality using inline optical and functional inspection tools

Nieves Espinosa,[a] Frank O. Lenzmann,[b] Stephen Ryley,[c] Dechan Angmo,[a] Markus Hösel,[a] Roar R. Søndergaard,[a] Dennis Huss,[d] Simone Dafinger,[d] Stefan Gritsch,[d] Jan M. Kroon,[e] Mikkel Jørgensen[a] and Frederik C. Krebs*[a]

Organic photovoltaic modules have been evaluated for their integration in mobile electronic applications such as a laser pointer. An evaluation of roll-to-roll processed indium and silver free polymer solar cells has been carried out from different perspectives: life cycle assessment, cost analysis and layer quality evaluation using inline optical and functional inspection tools. The polymer solar cells were fabricated in credit card sized modules by three routes, and several encapsulation alternatives have been explored, with the aim to provide the simplest but functional protection against moisture and oxygen, which could deteriorate the performance of the cells. The analysis shows that ITO- and silver-free options are clearly advantageous in terms of energy embedded over the traditional modules, and that encapsulation must balance satisfying the protection requirements while having at the same time a low carbon footprint. From the economic perspective there is a huge reduction in the cost of the ITO- and silver-free options, reaching as low as 0.25 € for the OPV module. We used inspection tools such as a roll-to-roll inspection system to evaluate all processing steps during the fabrication and analyse the layers' quality and forecast whether a module will work or not and establish any misalignment of the printed pattern or defects in the layers that can affect the performance of the devices. This has been found to be a good tool to control the process and to increase the yield.

Received 21st December 2012
Accepted 10th April 2013

DOI: 10.1039/c3ta01611k

www.rsc.org/MaterialsA

Introduction

Mobile as well as information and communications technology (ICT) applications that require electrical energy can be powered by a storage unit such as a battery or an energy-harvesting unit such as a solar cell. In typical applications, energy storage and energy harvesting devices operate together. Polymer solar cells have been contemplated as light harvesting devices for mobile and ICT applications for quite some time and have been demonstrated in some applications. In most of the examples they have been based on flexible polyester foil with indium-tin-oxide as the front electrode with the polymer solar cells being prepared initially by a combination of sheet-to-sheet and roll-to-roll processing. Today they are manufactured exclusively by roll-to-roll processing and sheet-to-sheet processing has no industrial or commercial value besides being a tool employed during initial development. Early life cycle analysis studies carried out by several independent groups[1–3] concluded that use of indium among other metals will not enable sustainable use of photovoltaic technologies due to barriers related to resource scarcity[4,5] resulting in high cost and environmental impact. Accordingly, replacements with a technical performance on par with ITO and that can be R2R compatible are being sought. There have been a few examples and most are based on metals such as copper or silver.[6–11] Regarding the technical performance, especially silver shows promise. Good processability is achievable for example as silver electrodes can be easily printed at high speed and in high yield. However, in terms of resource abundance, silver is as scarce as indium which implies that replacing indium with silver cannot be expected to be a valid solution.[4] Therefore new abundant electrode materials must be developed and even if silver could be recycled more easily than indium other alternatives such as the recently reported carbon-based electrodes[12,13] are highly attractive.

When analysing the potential of OPV for mobile and ICT applications, life cycle analysis in conjunction with cost analysis

[a]Department of Energy Conversion and Storage, Technical University of Denmark, Frederiksborgvej 399, DK-4000 Roskilde, Denmark. E-mail: frkr@dtu.dk

[b]ECN Solar Energy, P.O. Box 1, 1755 ZG Petten, The Netherlands

[c]UK Materials Technology Research Institute, Nottingham Road, Melton Mowbray, LE13 0PB, UK

[d]Dr. Schenk GmbH Industriemesstechnik, Einsteinstrasse 37, D-82152 Planegg, Germany

[e]ECN Solar Energy, High Tech Campus 5 (P-61), 5656 AE Eindhoven, The Netherlands

is an indispensable set of tools that can be used to direct the R&D efforts in such a way that compliance with desired economic and environmental boundary conditions is achieved. Since manufacturing yields can have a strong impact on environmental and cost calculations, the critical assessment of yields along the complete process chain is of vital importance. In line quality monitoring can be used for the optimization of yields as we also demonstrate in this present study.

In this work we report on the LCA and cost analysis of different OPV device structures for mobile electronic applications. Furthermore, we show how a high technical yield can be ensured by quality control using fast inline optical and functional inspection tools.

Methodology

Life cycle assessment

Since every aspect in the lifespan of a device can be assessed with life cycle assessment tools, from its conception to its end of life and even beyond, it is possible to guide the complete processing of any product towards a sustainable path. There have been a few LCA studies related to plastic solar cells from the lab scale[14,15] to the roll-to-roll production[3] in which critical parameters have been established. ITO has been estimated to embed from 66% to 87%[3,16] of the energy required for the materials, mainly due to its deposition *via* a sputtering process. Drying steps have been pointed out as energy intensive processes as well as layer thicknesses. Therefore a few alternatives that do not compromise efficiency but keep a low energy budget have been addressed in this study. An OPV powered demonstrator lamp was studied as well,[17,3] showing the great environmental advantage these devices can have over kerosene lamps and other light supply options. Based on these previous results, a new collection of routes for processing polymer solar cells addressing the hotspots was designed and assessed.

The scope of this life cycle analysis is to estimate the cradle-to-gate embodied energy associated with the production of polymer solar modules by three different routes with different encapsulation and adhesives. The goal is to assess the performance of these indium and silver free modules, which are meant to be used in laser pointer devices, and lead to a solution with lower environmental impact as well as faster reduction in manufacturing costs.

The quality of an LCA study is strongly correlated with the quality of the inventory data, therefore the first step to accomplish in every life cycle analysis[18] is to ensure the quality of the material and energy needs of the modules manufacturing. This step is known as Life Cycle Inventory (LCI) and it is made for a *functional unit* (FU), which is the amount of product that everything is calculated for. In this study the functional unit has been chosen as 1 m^2 of processed foil, where up to 161 credit card sized modules are produced. The reason for using this particular processed area originates from the fact that it has been a traditional unit used for PV, because it enables fair comparison with other PV technologies. It is moreover a very suitable unit for OPV modules fabricated by continuous methods, such as roll-to-roll techniques.

The commercial and widely used LCA software SimaPro (version 7.3.3) has been used in conjunction with its integrated Ecoinvent 2.2 database.[19] The embedded energy has been estimated by following the ISO 14040 standard Cumulative Energy Demand – CED V.1.04. Not all the inventory data required for this analysis are available from LCA databases such as the Ecoinvent database. For example, for the production of the materials for photoactive layers, adhesives or silver inks, inventory data had to be estimated from a publicly available literature, from public databases such as Bath Energy Inventory,[20] from contact with manufacturers, and from our own previous studies where embedded energies for some materials *e.g.* PEDOT:PSS, P3HT, PCBM, *etc.* were calculated.[3,14,15,21]

The energy requirements for every step in the manufacturing process of the solar cell devices were obtained by measurements at the pilot line facility. This is unlike other LCA studies, where energy consumption has been estimated from similar machinery, and sometimes leaving aside important processes such as drying,[14] so here real data from the machines used in the pilot line facility at DTU were used.

The Life Cycle Impact Assessment (LCIA) consists of the identification and evaluation of the amount and significance of the potential human and ecological effects arising from the LCI. Inputs and outputs obtained from the LCI, are classified and related to some environmental indicators, *e.g.* global warming potential (GWP), ozone layer depletion, *etc.*

For the combination of adhesive and encapsulation with the lowest embedded energy, we have introduced in SimaPro the processes and the environmental profile of each route evaluated. Environmental indicators have been estimated with SimaPro software by using the following methods:

- CML 2001 (baseline).
- Eco-indicator 99 (endpoint).

Life cycle costs of the different structures

The economic viability of OPV modules integrated in devices has been debated by some, although predicted future costs appear highly attractive. As an emerging technology OPV currently present a high cost when compared to other more established photovoltaic alternatives such as silicon or chalcogenides; in this study we want to emphasize the low share that the OPV modules present when viewed in terms of the overall device cost.

Although life cycle costing (LCC) has not yet been standardized officially at this moment, the following phases can be distinguished: goal and scope definition, cost calculations and interpretation of the results.

The goal and scope is to calculate the cost of a square meter of a polymer solar cell produced under the routes studied by LCA in this work.

The cost calculations in this study have a preliminary basis,[20] but since they have not been produced on a commercial scale so far, the costs of the materials, especially of those not produced on a bulk scale, are estimates. However, a detailed costs analysis of the manufacturing process has been possible through the extensive equipment for roll-to-roll processing available to this

project. In a PV system the cost should include materials and production costs of the modules as well as the balance of system component costs.

Inspection tools during processing and post processing

The quantitative analysis of the best solar cell stack with respect to costs and energy payback time is just one part of the device design. To ensure a full R2R production with high yield a qualitative inline analysis of each layer helps to identify processing defects and potential non-functional devices. A recently installed R2R optical inspection system (SolarInspect RtR, Dr Schenk GmbH, Germany) enables a 100% inspection of the moving substrate to detect point defects, layer homogeneity and misalignments of single layers and layer stacks. The system setup consists of three LED-based light sources (white, blue, red) with two 8192 pixel line-scan cameras, which can be used for the observation in the dark field, bright field, and transmission mode. The maximum web speed we explored in this work was 20 m min^{-1} while the system can be operated at much higher speeds. The maximum speed depends on the number of defects and ultrahigh speeds (>180 m min^{-1}) can only be reached for a relatively defect free material, as the data rate is what limits the web speed for optical inspection with high resolution. The device prepared here presented a high defect density and we ran the inspection at 2 m min^{-1} to ensure a proper data acquisition. The system has a detection resolution of down to 10 μm.

The devices were investigated as well using light beam induced current (LBIC) mapping of the final solar cell devices to identify the causes of poor performance. The performance of printable metal back electrodes for polymer solar cells has previously been investigated using LBIC.[22]

The LBIC experiments were carried out using a custom made setup with a 410 nm laser diode (5 mW output power, 100 μm spot size ≈ 65 W cm^{-2}, ThorLabs) mounted on a computer controlled *XY*-stage and focused to a spot size of <100 μm. The short circuit current from the device under study was measured using a computer controlled source measure unit (SMU, a Keithley 2400 model instrument).

Results and discussion

The mobile application as a subject of this study

To demonstrate the ITO-free technology, laser pointers in which the modules were integrated into a plastic rectangular body were fabricated.[23] Laser pointers comprising a solar cell module for charging a lithium ion polymer battery are shown in Fig. 1.

Fig. 1 A photograph of the application for the polymer solar cell modules studied here. A laser pointer comprising a solar cell module charging a lithium polymer ion battery. Three versions of the solar cell module designs were explored which differed in the choice of the electrode materials: An inkjet printed silver grid (front) and a silver back electrode = SSE (left), only a Pedot front and a silver back electrode = PSE (middle) and a module based on silver free electrodes = SFE utilizing all carbon modules (right).

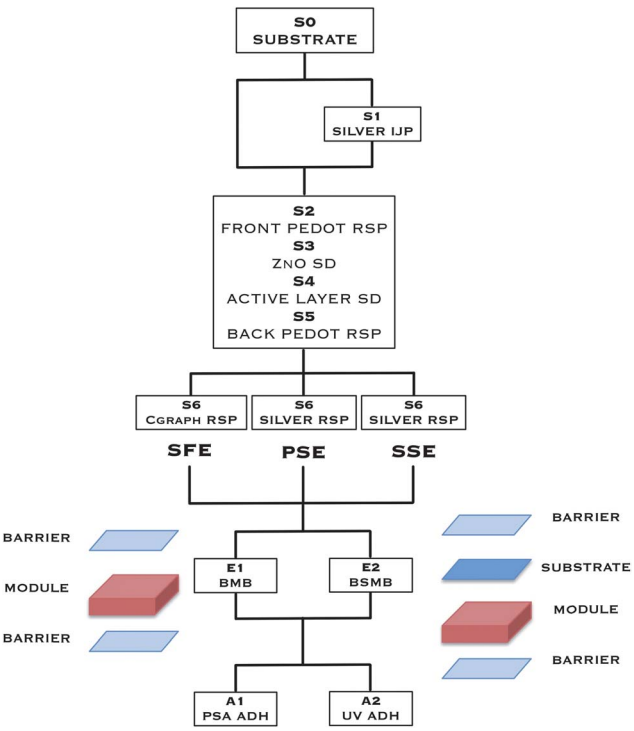

Fig. 2 The three routes, SFE, PSE and SSE, the encapsulation options – E1, E2 and the adhesive choices – A1, A2 analysed in this study.

Description of the process routes for the various solar cell designs

The versatility of the experimental setup for roll-to roll processing means that a variety of structures for the manufacturing of polymer solar modules can be produced as shown in Fig. 2. Three routes have been used with the purpose to be integrated in credit card size laser pointers, all comprising the same 4-layer stack in the core: PEDOT:PSS–ZnO–active–PEDOT:PSS, but varying the electrodes between silver and carbon graphite. The highly conductive front PEDOT:PSS (Heraeus Clevios PH1000) was diluted with isopropanol at a concentration of 10 : 3 (w/w), ZnO ink is a stabilized nanoparticle suspension in acetone (55 mg mL^{-1}) and the active layer comprised a solution of P3HT:PCBM (P3HT was Sepiolid P200 from BASF and PCBM was technical grade [60]PCBM from Solenne BV) in chlorobenzene (30 mg mL^{-1} each). The back PEDOT:PSS electrode

(Orgacon EL-P 5010 from Agfa) was diluted with isopropanol in a ratio of 10 : 2 (w/w).

For this core, processing was as follows: in the same in line machinery the first two layers are printed. First, front PEDOT:PSS is deposited by rotary screen printing, at 10 m min^{-1}, and dried at 140 °C in a 2 m length oven plus infrared light. The coating of the ZnO layer comes immediately after by slot-die at the same speed but dried at 90 °C in a 2 m length oven plus at 140 °C in a 2 m length oven. Separately in another run, the active layer is slot die coated at 5 m min^{-1} and dried at 140 °C in a 4 m length oven. To finish the core, top PEDOT:PSS is rotary screen printed at 2 m min^{-1} and dried after at 140 °C in a 2 m length oven plus infrared light. The electrodes in the modules define the three different routes as follows:

- In the Silver Free Electrode route (SFE) the back electrode is made with carbon graphite, patterned in a way that enables serial connections between stripes. This carbon ink was applied by rotary screen printing at 3 m min^{-1} speed and dried at 140 °C.

- To confirm the convenience of the use of carbon graphite as an electrode, the second route, named as Pedot Silver Electrodes (PSE), has silver printed at the backside in a pattern allowing for serial connections of the stripes. This was deposited by rotary screen printing at 2 m min^{-1} and dried at 140 °C.

- Modules with silver in both the front and the backside were used in what has been called Silver Silver Electrodes (SSE).[23] A water-based ink with a 20% silver loading was employed (Suntronic U7089 from Sun Chemicals) as front silver. Inkjet printing was carried out by printing directly on the substrate, followed by drying. The back silver electrode was rotary screen printed at 2 m min^{-1} followed by drying.

The encapsulation schemes in the benchmark devices of this study are based on either a "cold lamination" procedure using pressure sensitive adhesives (PSA), called A1 or using ultraviolet light curable adhesives (UVA), named A2. Modules with two alternative encapsulation structures have been fabricated as well: E1 consisting of barrier/module/barrier and E2 barrier/substrate/module/barrier, where PET foil is purchased as Melinex ST506 from Dupont–Teijin and the barrier material purchased from Amcor. While in the first encapsulation E1 structure, thin PET foils with basic moisture barrier properties may be sufficient for relatively short-lived mobile electronic applications, power generation applications are expected to require substantially different encapsulation schemes providing a more robust protection from humidity and oxygen ingress as well as from mechanical impacts. However, this consideration is not supposed to suggest that this is indeed the encapsulation structure for viable power generating OPV devices in the future; it will depend on the stability and degradation lifetimes.

The active area of all the modules is 45.5%, as a result of the several pattern limitations in each deposition step. Common steps and the flow of manufacturing the credit card size modules are shown in Fig. 2. All the three routes analysed here share steps from S2 to S5, from front PEDOT:PSS to back PEDOT:PSS deposition.

Life cycle analysis of the different device structures

Tables 1–3 show the material and energy inventories for 1 m^2 of the processed area with 161 modules produced. The material requirements in mass units (g) for the three routes have been either measured *in situ* or calculated directly from data sheets – from geometry calculations, *i.e.* pumping rates, wet thicknesses, mesh specifications, *etc.* They are given in Table 1.

With regard to the energy requirements, we distinguish here between two types: the energy required for the production of every input material used in the module manufacture, called *Materials Energy* (ME in Table 2), and the energy needed for operating the machines, called here *Direct Process Energy* (or DPE in Table 3).

One observation that can be made on the basis of the inventory in Table 2 is that for modules which are printed on PET and encapsulated with two barrier layers, the fraction of PET in the materials energy raises from 30% up to more than 50% (see a labelled shares in Fig. 3). The embodied energy of materials labelled with the letters b to k in Fig. 3 remains constant (11.82 MJ_{EPE}), which corresponds to fractions between 50 and 30% for the various designs.

For all routes and choices we have the same energy consumption for the manufacturing steps S2 to S5 (which are identical for all devices). These processing steps account for 9.60 MJ_{EPE}. The embodied energy of the other manufacturing steps (S1, S6 and S7) varies between the different devices as can be seen in Fig. 4–6. The figures show clearly, that back electrode printing (S6) contributes to a large part of the Direct Process Energy (DPE) in all cases. The manufacturing steps S1 and S7 on the other hand have only a negligible influence on the total manufacturing energy. The deposition of the back PEDOT:PSS layer (S5) contributes to the total DPE with a value of approx. 30% and the active layer deposition (S4) with approximately 16%.

Fig. 7 shows a comparison of the devices with the 3 different choices in electrode materials (SSE, PSE and SFE) in terms of the overall embedded energy (broken down into totals of materials energy and process energy) with the benchmark ITO-based module. S4, S5 and S6 are the slowest processes (5, 2 and 2/3 m min^{-1}) and correspondingly the drying processes raise the embedded energy, as indicated in Table 3. The lightest encapsulation structure based on the pressure sensitive adhesive was assumed in this figure. The silver free electrode route results in the lowest total embedded energy. In fact the value of only 37.58 MJ_{EPE} per m^2, is the lowest published for any organic photovoltaic device to date. For the energy embedded just in the ITO module, we have plotted a maximum value derived from a maximum energy embedded of 266.13 MJ_{EPE} m^{-2} and a minimum energy required of 130 MJ_{EPE} m^{-2} – total energies respectively shown in Fig. 7 – 291.42 and 155.29 MJ_{EPE} m^{-2}. The ratio between materials energy and direct energy has changed dramatically, from being 30/70 to be more balanced 40/60 approximately. Moreover, the carbon-based new route shows a decrease in energy of a factor of 10 times.

Table 1 Material inventory in grams for the processing of 1 m^2 by the three routes analysed: SFE, PSE and SSE, with the two encapsulation options and using two different adhesives

	E1 A1			E2 A1			E1 A2			E2 A2		
	SFE	PSE	SSE	SFE	PSE	SSE	SFE	PSE	SSE	SFE	PSE	SSE
S0 substrate												
PET film	—	—	—	178.10	178.10	178.10	—	—	—	178.10	178.10	178.10
PSA	—	—	—	10.12	10.12	10.12	—	—	—	—	—	—
UVA	—	—	—	—	—	—	—	—	—	14.00	14.00	14.00
Barrier	65.48	65.48	65.48	65.48	65.48	65.48	65.48	65.48	65.48	65.48	65.48	65.48
S1 front electrode IJP												
Silver ink	—	—	0.09	—	—	0.09	—	—	0.09	—	—	0.09
S2 Pedot deposition												
PEDOT:PSS	26.32	26.32	26.32	26.32	26.32	26.32	26.32	26.32	26.32	26.32	26.32	26.32
Isopropanol	7.90	7.90	7.90	7.90	7.90	7.90	7.90	7.90	7.90	7.90	7.90	7.90
S3 ZnO deposition												
Zinc acetate	0.29	0.29	0.29	0.29	0.29	0.29	0.29	0.29	0.29	0.29	0.29	0.29
Potassium hydroxide	0.20	0.20	0.20	0.20	0.20	0.20	0.20	0.20	0.20	0.20	0.20	0.20
Methanol	2.60	2.60	2.60	2.60	2.60	2.60	2.60	2.60	2.60	2.60	2.60	2.60
Acetone	5.20	5.20	5.20	5.20	5.20	5.20	5.20	5.20	5.20	5.20	5.20	5.20
Methoxyethoxy acetic acid	0.04	0.04	0.04	0.04	0.04	0.04	0.04	0.04	0.04	0.04	0.04	0.04
S4 active layer												
P3HT	0.10	0.10	0.10	0.10	0.10	0.10	0.10	0.10	0.10	0.10	0.10	0.10
PCBM	0.08	0.08	0.08	0.08	0.08	0.08	0.08	0.08	0.08	0.08	0.08	0.08
Chlorobenzene	7.28	7.28	7.28	7.28	7.28	7.28	7.28	7.28	7.28	7.28	7.28	7.28
S5 back PEDOT												
PEDOT:PSS ink	33.05	33.05	33.05	33.05	33.05	33.05	33.05	33.05	33.05	33.05	33.05	33.05
S6 back electrode												
Carbon graphite	5.14	—	—	5.14	—	—	5.14	—	—	5.14	—	—
Silver ink	—	7.61	7.61	—	7.61	7.61	—	7.61	7.61	—	7.61	7.61
S7 encapsulation												
PSA	6.97	6.97	6.97	6.97	6.97	6.97	—	—	—	—	—	—
UVA	—	—	—	—	—	—	9.64	9.64	9.64	9.64	9.64	9.64
Barrier	45.08	45.08	45.08	45.08	45.08	45.08	45.08	45.08	45.08	45.08	45.08	45.08
Total mat. inventory (g)	205.71	208.18	208.28	393.93	396.40	396.50	208.38	210.85	210.95	400.48	402.95	403.05

Encapsulation and adhesive choices impact

To prevent moisture and oxygen entering the devices, these are encapsulated in a final step. When the modules are directly printed on the barrier material, just another barrier layer is laminated on top (E1). But when they are printed on the PET substrate, the barrier material is laminated on both sides, front and back or bottom and top. This last option, E2 has a strong impact on the materials energy, since it means an extra layer; going in the case of the SFE route from 23.04 to 39.45 MJ_{EPE} per FU.

When analysing the two adhesives that have been used to glue the barrier material to the modules, one of them, the PSA embeds less energy both in the material production itself and in the processing of the OPV modules. The UV curable adhesive has stronger bond strength but requires 6 kW power of UV light for crosslinking meaning around 2.5 MJ_{EPE} more energy embedded. This latter point can possibly be optimized by employing LED lamps with emission spectra specifically suited for curing the adhesive. We estimate that the same curing efficiency can be achieved with around 2 kW of LED power.

Assessment of other environmental impact categories

Table 4 shows the results of the LCA calculations for other environmental impact categories, *i.e.*, non-renewable energy use (NREU), climate change in the next 100 years (global warming potential, GWP100), abiotic depletion, ozone layer depletion, photochemical oxidant formation, acidification and eutrophication. The calculation of environmental impacts (except NREU) follows the latest CML method.

In Fig. 8 further illustrations of the environmental impact calculations are shown. Eco-indicator values indicate a material's or an action's impact based on its effects on the different categories chosen. One conclusion that can be drawn from these illustrations, for example, is that the SFE route does not cause any impact on carcinogens since it does not involve the use of silver.

Table 2 Materials energy inventory in MJ of equivalent primary energy units for the processing of 1 m^2 by the three routes analysed: SFE, PSE and SSE, with the two encapsulation options and using two different adhesives

	E1 A1			E2 A1			E1 A2			E2 A2		
	SFE	PSE	SSE	SFE	PSE	SSE	SFE	PSE	SSE	SFE	PSE	SSE
PET	8.93	8.93	8.93	23.31	23.31	23.31	8.93	8.93	8.93	23.31	23.31	23.31
PEDOT:PSS	9.46	9.46	9.46	9.46	9.46	9.46	9.46	9.46	9.46	9.46	9.46	9.46
Isopropanol	0.50	0.50	0.50	0.50	0.50	0.50	0.50	0.50	0.50	0.50	0.50	0.50
P3HT	0.18	0.18	0.18	0.18	0.18	0.18	0.18	0.18	0.18	0.18	0.18	0.18
PCBM	0.87	0.87	0.87	0.87	0.87	0.87	0.87	0.87	0.87	0.87	0.87	0.87
Chlorobenzene	0.45	0.45	0.45	0.45	0.45	0.45	0.45	0.45	0.45	0.45	0.45	0.45
$Zn(OAc)_2$	0.01	0.01	0.01	0.01	0.01	0.01	0.01	0.01	0.01	0.01	0.01	0.01
KOH	0.01	0.01	0.01	0.01	0.01	0.01	0.01	0.01	0.01	0.01	0.01	0.01
MeOH	0.10	0.10	0.10	0.10	0.10	0.10	0.10	0.10	0.10	0.10	0.10	0.10
Acetone	0.24	0.24	0.24	0.24	0.24	0.24	0.24	0.24	0.24	0.24	0.24	0.24
MEA	0.00	0.00	0.00	0.00	0.00	0.00	0.00	0.00	0.00	0.00	0.00	0.00
Carbon graphite	0.90			0.90			0.90			0.90		
Silver ink		2.35	2.38		2.35	2.38		2.35	2.38		2.35	2.38
Pressure sensitive adhesive	1.40	1.40	1.40	3.43	3.43	1.40						
UV curable adhesive							1.93	1.93	1.93	4.74	4.74	4.74
Subtotal (MJ_{EPE})	23.04	24.50	24.53	39.45	40.91	40.94	23.58	25.03	25.06	40.77	42.22	42.25

Table 3 Energy inventory in MJ of equivalent primary energy units for the processing of 1 m^2 by the three routes analysed: SFE, PSE and SSE, with the two encapsulation options and using two different adhesives. The conversion factor used for primary energy to electricity is 35%

	E1 A1			E2 A1			E1 A2			E2 A2		
	SFE	PSE	SSE	SFE	PSE	SSE	SFE	PSE	SSE	SFE	PSE	SSE
S0 substrate												
R2R lamination	—	—	—	0.04	0.04	0.04	—	—	—	2.53	2.53	2.53
S1 front electrode IJP												
Silver ink	—	—	0.08	—	—	0.08	—	—	0.08	—	—	0.08
Layer drying			1.90			1.90			1.90			1.90
S2 front Pedot deposition by RSP												
PEDOT:PSS deposition	0.12	0.12	0.12	0.12	0.12	0.12	0.12	0.12	0.12	0.12	0.12	0.12
Layer drying	0.70	0.70	0.70	0.70	0.70	0.70	0.70	0.70	0.70	0.70	0.70	0.70
S3 ZnO deposition by SD												
ZnO ink preparation	0.40	0.40	0.40	0.40	0.40	0.40	0.40	0.40	0.40	0.40	0.40	0.40
ZnO coating	0.08	0.08	0.08	0.08	0.08	0.08	0.08	0.08	0.08	0.08	0.08	0.08
Layer drying	0.59	0.59	0.59	0.59	0.59	0.59	0.59	0.59	0.59	0.59	0.59	0.59
S4 active layer deposition by SD												
P3HT:PCBM ink preparation	0.07	0.07	0.07	0.07	0.07	0.07	0.07	0.07	0.07	0.07	0.07	0.07
P3HT:PCBM coating	0.28	0.28	0.28	0.28	0.28	0.28	0.28	0.28	0.28	0.28	0.28	0.28
Layer drying	2.36	2.36	2.36	2.36	2.36	2.36	2.36	2.36	2.36	2.36	2.36	2.36
S5 Back PEDOT:PSS by RSP												
PEDOT:PSS printing	0.59	0.59	0.59	0.59	0.59	0.59	0.59	0.59	0.59	0.59	0.59	0.59
Layer drying	4.07	4.07	4.07	4.07	4.07	4.07	4.07	4.07	4.07	4.07	4.07	4.07
S6 back electrode printing by RSP												
Carbon/silver ink printing	0.39	0.59	0.59	0.39	0.59	0.59	0.39	0.39	0.39	0.39	0.39	0.39
Layer drying	4.50	6.74	6.74	4.50	6.74	6.74	4.50	6.74	6.74	4.50	6.74	6.74
S7 encapsulation												
R2R lamination	0.04	0.04	0.04	0.04	0.04	0.04	0.04	0.04	0.04	0.04	0.04	0.04
Total	14.54	16.98	18.96	14.58	17.02	19.00	17.02	17.02	21.45	19.55	22.00	23.98

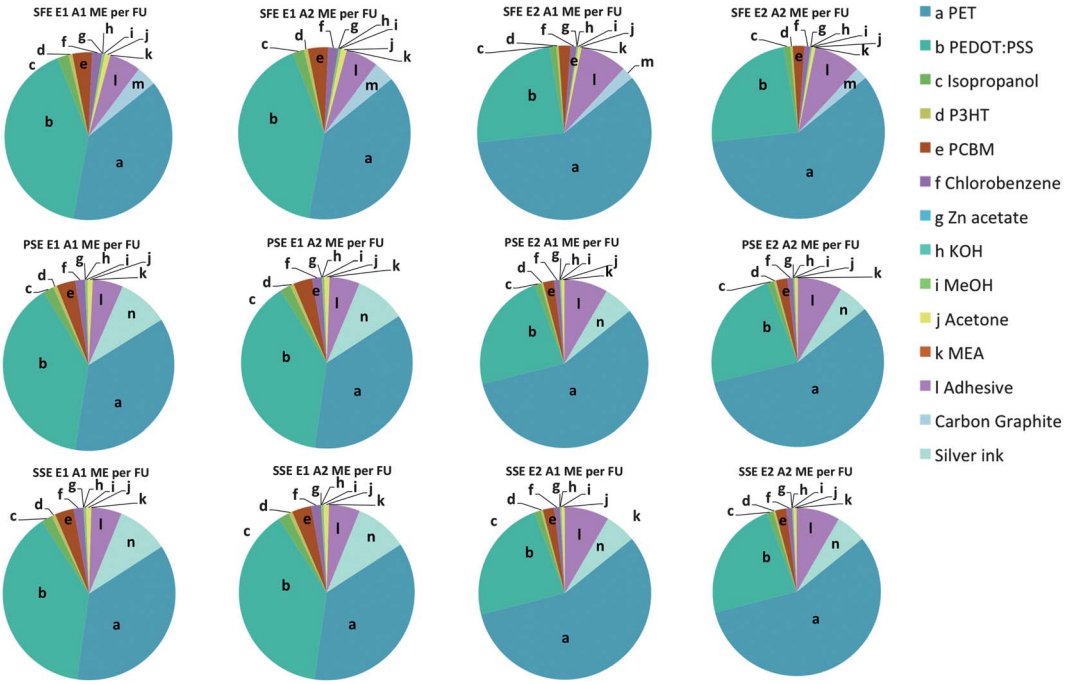

Fig. 3 Material energy requirements share for the different routes with two encapsulation and two adhesive choices per functional unit (FU).

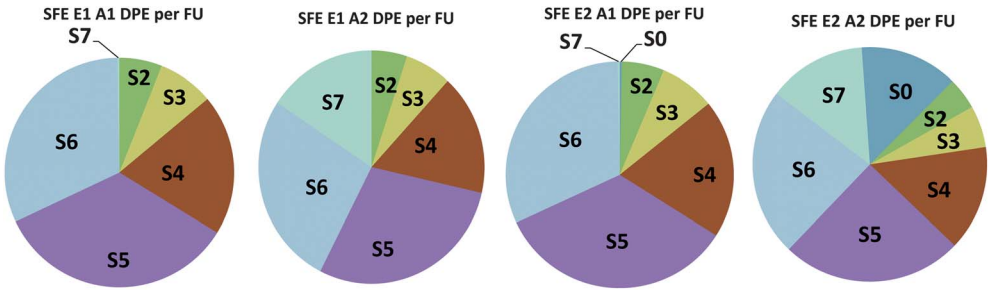

Fig. 4 Energy share used in the OPV modules manufacturing steps, from S1 to S7, for the SFE route with four encapsulation and adhesive choices; *i.e.* E1, E2, A1, and A2.

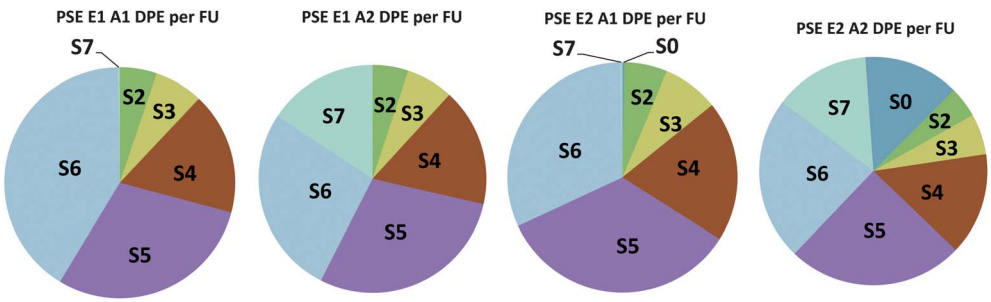

Fig. 5 Energy share used in the OPV modules manufacturing steps, from S1 to S7, for the PSE route with four encapsulation and adhesive choices; *i.e.* E1, E2, A1, and A2.

Energy payback time (EPBT) and energy return factor (ERF)

For an energy-production technology and especially for renewable energy technologies, it is of great value that the system quickly re-generates the equivalent amount of energy consumed in its construction and decommissioning phases. And that this is done several times along its lifetime (L). These concepts are reflected by the parameters energy pay-back time (EPBT) and energy return factor (ERF). EPBT and ERF are defined in eqn (1) and (2) below.

$$\mathrm{EPBT} = \frac{E_{\mathrm{EMB}}}{E_{\mathrm{GEN}}} \quad (1)$$

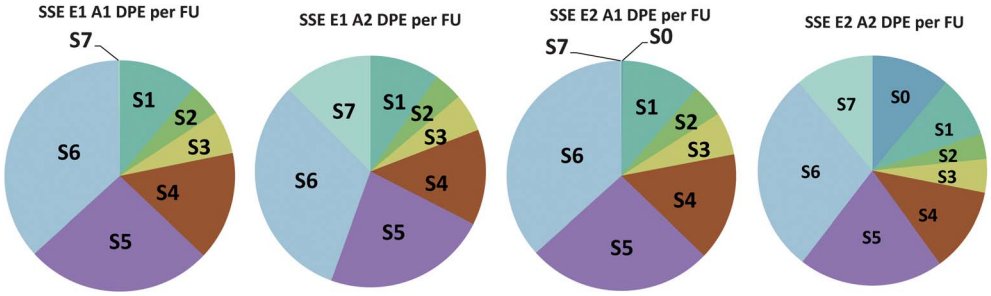

Fig. 6 Energy share used in the OPV modules manufacturing steps, from S1 to S7, for the SSE route with four encapsulation and adhesive choices; *i.e.* E1, E2, A1, and A2.

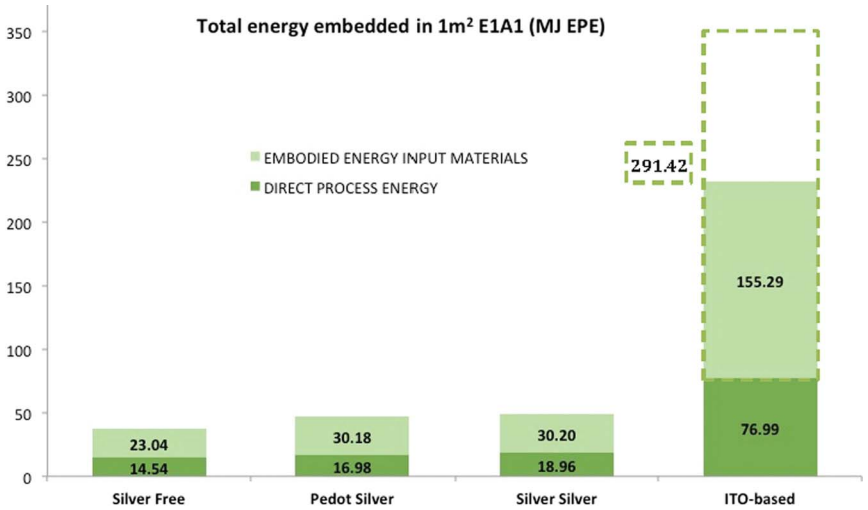

Fig. 7 Total embedded energy comparison of 1 functional unit of 1 m^2 ITO-based modules – with maximum and minimum values – and the modules manufactured by the three routes directly printed on the barrier – E1 – and using pressure sensitive adhesive from 3M™ – A1.

Table 4 LCA results for 1 m^2 of polymer solar modules manufactured by the three routes SFE, PSE, SSE for E1 and A1 choices

Results for 1 m^2 processed area				
Environmental impact category	Unit	SFE	PSE	SSE
NREU	MJ	37.58	41.48	43.49
Climate change	g CO_2 eq.	2350	3222	3440
Abiotic depletion	g Sb eq.	0.0203	0.0525	0.0537
Ozone layer depletion	g CFC-11 eq.	1.26×10^{-7}	1.88×10^{-7}	1.94×10^{-7}
Photochemical oxidant formation	g ethene	0.000441	0.00104	0.00106
Acidification	g SO_2 eq.	0.00762	0.0248	0.0253
Eutrophication	g PO_4^3 eq.	0.00188	0.0242	0.0246

$$\mathrm{ERF} = \frac{E_{\mathrm{GEN}} L}{E_{\mathrm{EMB}}} = \frac{L}{\mathrm{EPBT}} \quad (2)$$

They can be determined from the total embodied energy (E_{EMB}) and the electricity output (E_{GEN}) of the OPV module as defined further above. It is not the purpose of the laser pointers to create energy, however, if the modules were used for that, they would have energy payback times in the range of less than 4 months in the case of the silver free electrode route. Results are gathered in Table 5.

Cost analysis of the different device structures

Building on the detailed material inventory shown in Table 1 and the manufacturing process explained in the previous section, the economic cost of a 1 m^2 organic photovoltaic system has been calculated taking into account the materials, direct process, balance of system component costs and using a well established methodology for the economic analysis.[24,25] Costs of materials involved in the modules manufacturing such as inks and solvents are their price as purchased from the suppliers. Production costs have been determined for the manufacturing steps, and included in Table 6, as the electricity consumption of the machinery (using a cost of industry electricity typical for Europe of 0.116 € per kW h (ref. 26)).

The material costs for every route and encapsulation choice are shown in Table 6. The total cost varies between 41.77 € per m^2 and 69.47 € per m^2 for the various devices. It might seem a high cost for a gadget, but for the use of these OPV modules in energy systems, this would be a reasonable price of ex-factory cost of 0.25 € per device, representing a low share.

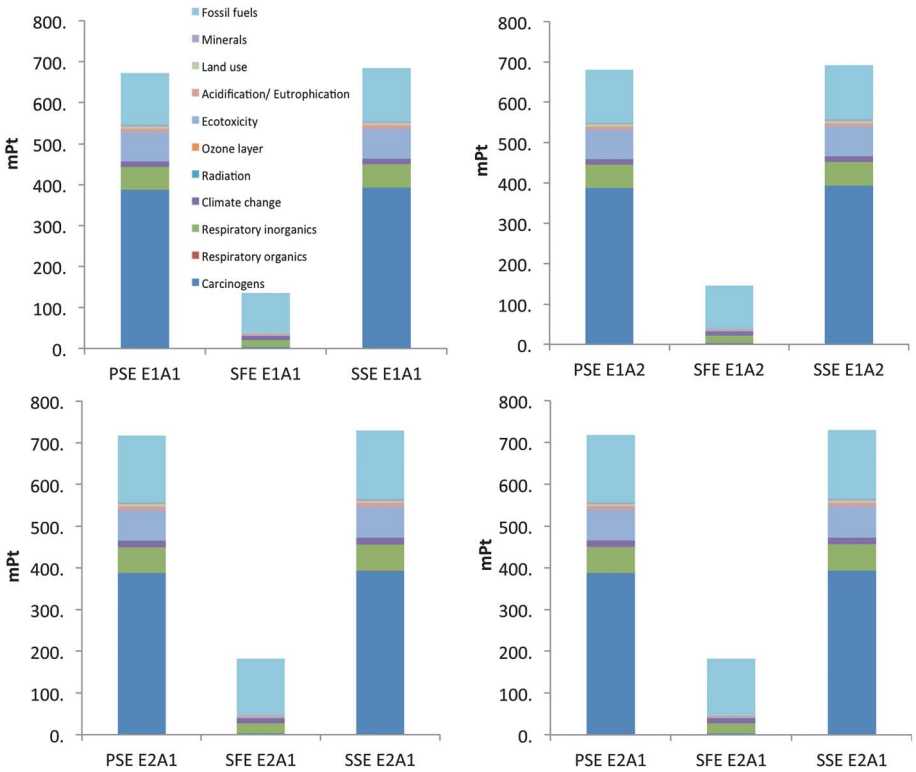

Fig. 8 Comparing 'PSE', 'SFE' and 'SSE' routes with the method: Eco-indicator 99 (E) V2.07/Europe EI 99 E/E/Single score. SimaPro, pRé Consultants, The Netherlands.

Table 5 Energy payback times and energy return factors for 1 m^2 processed surface of OPV modules prepared by the three routes, the subject of this study, for 2% efficiency and 45.53% of active area, and assuming an insolation level of 1700 kW h m^{-2} per year

	E1 A1			E2 A1			E1 A2			E2 A2		
	SFE	PSE	SSE	SFE	PSE	SSE	SFE	PSE	SSE	SFE	PSE	SSE
EPBT (years)	0.29	0.33	0.34	0.42	0.45	0.47	0.32	0.35	0.37	0.47	0.50	0.52
EPBT (months)	3.54	3.91	4.10	5.09	5.46	5.65	3.82	4.19	4.38	5.68	6.05	6.24
ERF	50.85	46.07	43.94	35.37	32.98	31.88	47.06	42.94	41.08	31.68	29.75	28.85

The photoactive and electrode layers hardly have, however, any significant contribution to the costs, due to the fact that the layers are very thin. While in previous ITO-based modules this transparent conductor represented a 37%[29] share of the total cost; now most of the cost is attributed to the back PEDOT:PSS, representing 40% in some cases, but moreover adding both front and back PEDOT:PSS, the share raises up to 60%, as shown in Fig. 9. It is very curious that the majority of the cost is driven by the materials in the new set of routes – more than 99% of the cost is due to the materials, while the cost of the electricity for processing is insignificant.

Performing a limited comparison with other PV technologies, it appears that per W_p of OPV module, the ex-factory costs are 5 times higher than the ex-factory costs of thin film amorphous silicon PV modules, *i.e.* €5.57 per W_p *versus* €1.1 per W_p.[27] According to currently published EU average electricity price for households is €0.19 per kW h,[28] and considering an internal rate of return of more than 20%, the price of the OPV product for a rollup charging panel must be not more than €1.70 per W_p. Here, from our study the significant costs come from the PEDOT:PSS layers, caused by a high unit price, compared to the other materials. We can expect reductions in price if economies of scale are considered and PEDOT:PSS is produced in bulk.

Assuming values for the performance ratio of the PV system, insolation level, inflation and interest rates, the levelized cost of electricity (LCOE) from an organic photovoltaic system has been calculated to be 0.26 € per kW h for 3% efficiency modules with a 5 years lifetime, a performance ratio of 0.85 and an insolation of 1700 kW h m^{-2} per year.[29]

In-line optical inspection

All of the analyses above assume a technical yield of 100% which is of course unrealistic while it is possible to achieve such a very high technical yield using in-line inspection during manufacture. In this study we employed a R2R inspection system as shown in Fig. 10 to analyse all processing steps during the fabrication of the

Table 6 Material cost of 1 m^2 of the processed surface in € manufactured by the three routes analysed: SFE, PSE and SSE, with the two encapsulation options and using two different adhesives

	SFE				PSE				SSE			
Material	E1 A1	E2 A1	E1 A2	E2 A2	E1 A1	E2 A1	E1 A2	E2 A2	E1 A1	E2 A1	E1 A2	E2 A2
PET substrate	—	2.84	—	2.84	—	2.84	—	2.84	—	2.84	—	2.84
Barrier	5.95	11.90	5.95	11.90	5.95	11.90	5.95	11.90	5.95	11.90	5.95	11.90
Adhesive												
Pressure sensitive	1.76	4.31	—	—	1.76	4.31	—	—	1.76	4.31	—	—
UV curable	—	—	5.82	14.28	—	—	5.82	14.28	—	—	5.82	14.28
Carbon graphite	0.30	0.30	0.30	0.30								
Silver												
IJP	—	—	—	—	—	—	—	—	0.20	0.20	0.20	0.20
RSP	—	—	—	—	6.37	6.37	6.37	6.37	6.37	6.37	6.37	6.37
PEDOT												
Front	8.55	8.55	8.55	8.55	8.55	8.55	8.55	8.55	8.55	8.55	8.55	8.55
Back	16.52	16.52	16.52	16.52	16.52	16.52	16.52	16.52	16.52	16.52	16.52	16.52
P3HT	2.69	2.69	2.69	2.69	2.69	2.69	2.69	2.69	2.69	2.69	2.69	2.69
PCBM	4.31	4.31	4.31	4.31	4.31	4.31	4.31	4.31	4.31	4.31	4.31	4.31
$Zn(OAC)_2$	0.59	0.59	0.59	0.59	0.59	0.59	0.59	0.59	0.59	0.59	0.59	0.59
Solvents												
Chlorobenzene	0.57	0.57	0.57	0.57	0.57	0.57	0.57	0.57	0.57	0.57	0.57	0.57
Isopropanol	0.19	0.19	0.19	0.19	0.19	0.19	0.19	0.19	0.19	0.19	0.19	0.19
Acetone	0.13	0.13	0.13	0.13	0.13	0.13	0.13	0.13	0.13	0.13	0.13	0.13
MeOH	0.05	0.05	0.05	0.05	0.05	0.05	0.05	0.05	0.05	0.05	0.05	0.05
KOH	0.01	0.01	0.01	0.01	0.01	0.01	0.01	0.01	0.01	0.01	0.01	0.01
MEA	0.00	0.00	0.00	0.00	0.00	0.00	0.00	0.00	0.00	0.00	0.00	0.00
Subtotal (€)	41.61	52.95	45.68	62.92	47.68	59.02	51.75	68.99	47.88	59.22	51.95	69.20
Electricity cost (€)	0.16	0.16	0.19	0.22	0.19	0.19	0.22	0.25	0.21	0.21	0.24	0.27
Total (€)	41.77	53.11	45.87	63.15	47.87	59.21	51.97	69.24	48.09	59.43	52.19	69.47

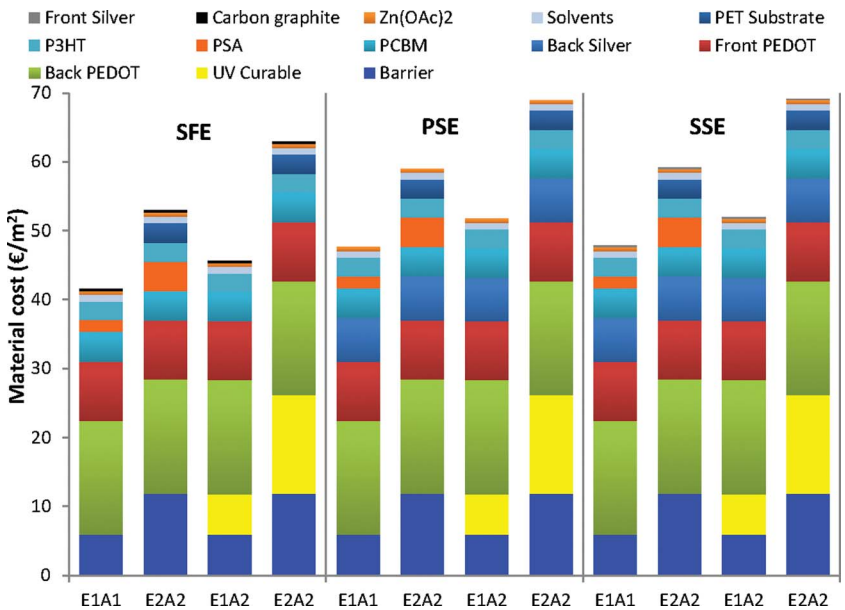

Fig. 9 Materials cost in € per m^2 of the processed substrate for all the encapsulation choices and manufacturing routes.

ITO and silver free devices with carbon back electrodes. Each of the three illumination modes was used to evaluate its suitability on the increasing layer stack. An overview of the camera output and the detection quality for each mode is shown in Fig. 11.

Bright field and transmission mode is best suited for thin and semi-transparent layers such as the first PEDOT:PSS electrode and the ZnO layer. The slight inhomogeneity due to the screen printing of the PEDOT:PSS layer is clearly visible. The

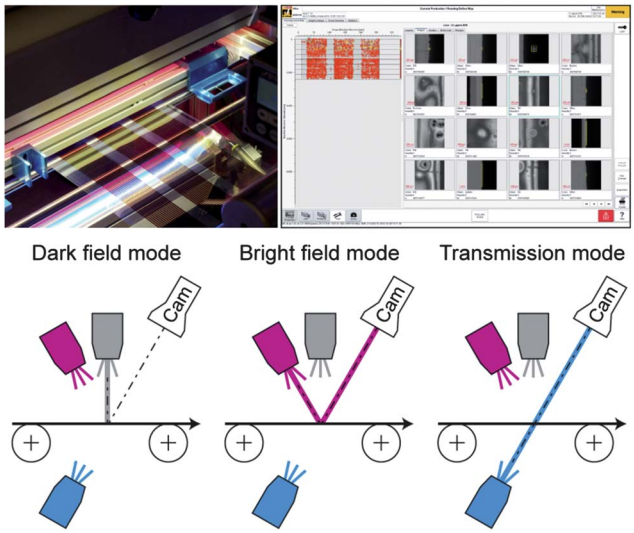

Fig. 10 Photograph of the optical R2R inline inspection system (top left) and the corresponding graphical user interface of the inspection software showing a real-time defect map (top right). The principal setup with three different illumination modes is illustrated below.

effect on the solar cell performance is negligible, whereas pinholes will act as zones without current generation. The stacked layer of PEDOT:PSS with ZnO and even the active layer can be inspected in the best way with the bright field mode. Optical fringes due to different layer thicknesses or around pinholes help to identify potential zones of short cuts in the final device. Pinholes can easily be detected in the transmission mode for thick and less transparent layers where they show up as white spots. It shows a low suitability for the full layer stack as everything shows up black. The several layers and their alignments are hard to differentiate.

The dark field mode is preferably used for thick and rough surfaces such as the back PEDOT:PSS and the carbon electrode on top of the layer stack. Hereby the edge quality, pinholes and a functional serial interconnection are the main areas of inspection.

The optical inspection is a very good tool to map the complete substrate with all fabricated modules on it. It helps to analyse the layer quality and defects for potential process optimizations to ensure a high production yield. Furthermore, it is possible to identify areas with non-functional devices due to misalignment leading to short cuts. These areas can be

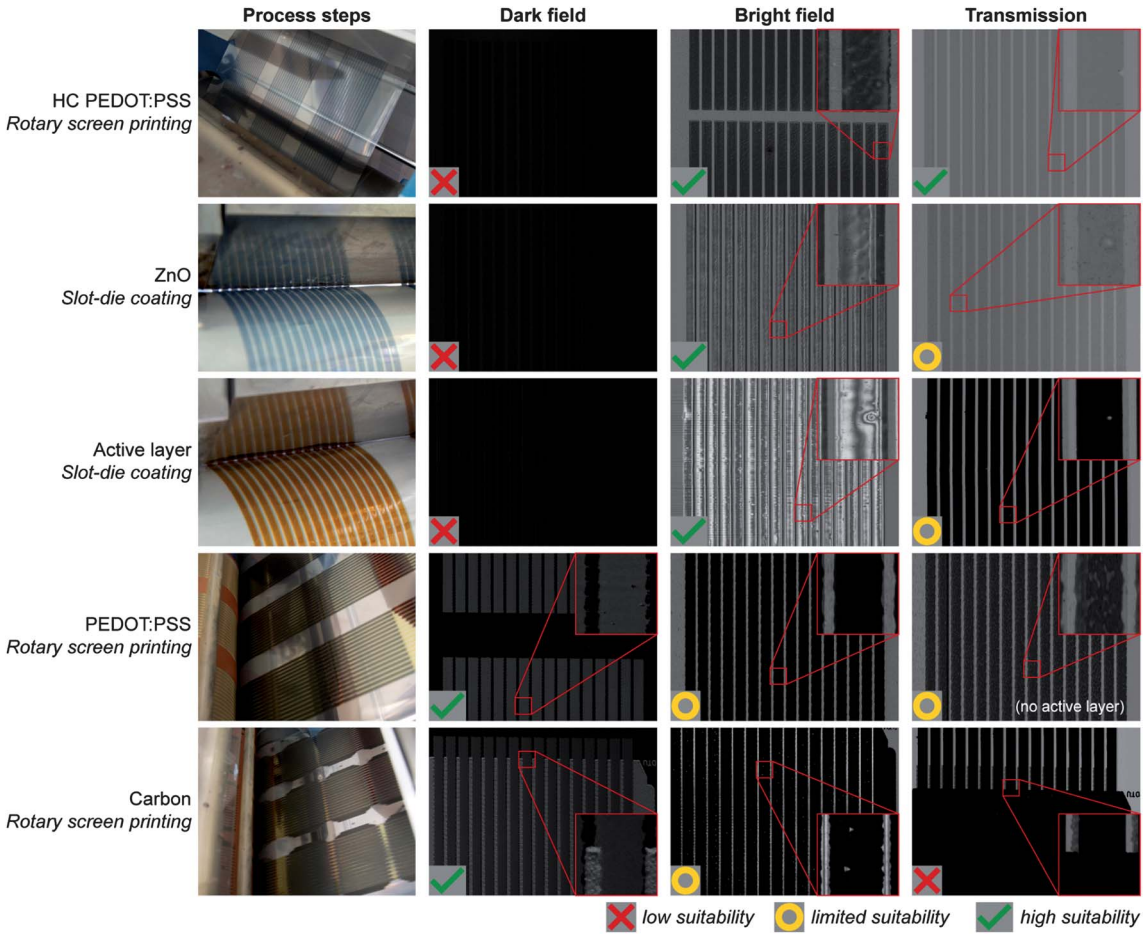

Fig. 11 Suitability of the three illumination modes for the different materials on the layer stack. Each mode has advantages and disadvantages depending on the printed material and on the stack size.

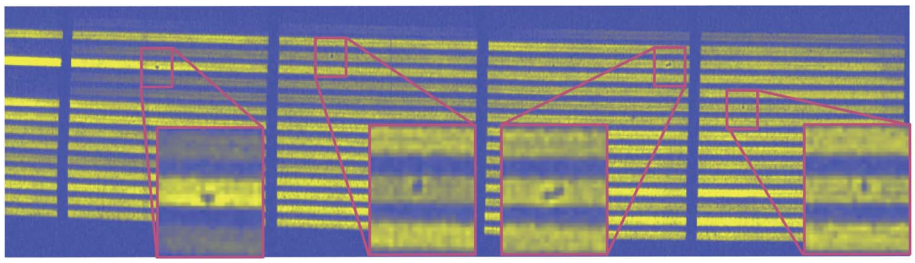

Fig. 12 LBIC images of several completed devices in the same region of the web, with carbon graphite electrodes where dust particles and dewetting spots can be observed – some are magnified.

extracted from subsequent handling processes such as lamination and device integration to increase the overall production efficiency.

Functional inspection post processing

With the LBIC technique, defects and thickness variations due to the R2R coating processes are most easily seen for the cells with fully covering electrodes, as in Fig. 12. There can be seen small dark spots that may originate point defects. This type of defects could arise from either bubbles in one of the coating solutions or from point defects in a layer beneath that inhibits coating causing dewetting in the subsequent one. These defects, however, do not always catastrophically impede the overall functioning of the cell but may result in partial device shunting and cause a lower fill factor. Weaker lines and areas that are seen to run along the R2R stripe pattern may be due to thickness variations inherent in this type of coating process.

Conclusions

The sought replacement of ITO as an electrode in organic photovoltaics has been fulfilled in this work. First attempts with silver have resulted in an affordable option in terms of cost and environmental impact. However, forecasting a larger scale of OPV modules and attending to the availability of material resources, silver is unlikely to represent the right choice for replacing indium. Therefore the use of carbon inks as employed here has been proven to be a more sustainable as well as affordable option. The use of silver and indium free OPV modules, especially for this kind of applications, provide significant advantages in their profile to be a cheap and green product easy to integrate and dispose; opening up opportunities for exclusive access to particular markets.

Several encapsulation structures for the modules in the devices have been presented and their analyses reveal the importance of the substrate and encapsulation components choice on the overall environmental profile. The pressure sensitive adhesive embeds less energy both in the material production itself and in the processing of the OPV modules as compared to the UV curable adhesive. The UV curing adhesive offers a better encapsulation but requires high power of UV light for cross-linking, meaning 20% more energy embedded on average.

The cost of electricity from an organic photovoltaic system could be more favourable than that obtained for an equivalent inorganic (silicon-based) system and could attain grid parity in the coming years. Nevertheless, for a long-term perspective the prospected manufacturing costs in terms of € per m^2, are not sufficient. There is still a need to increase efficiency and lifetime substantially to become really competitive with c-Silicon technologies.

Besides such environmental and cost analyses, to ensure the high yield of a full R2R production, a qualitative inline analysis of each layer has been performed to identify processing defects and potential non-functional devices. On the one hand, a R2R optical inspection system by Dr. Schenk GmbH that enables a 100% inspection of the moving substrate was employed. On the other hand, the LBIC technique mapping the current was used for functional testing. Both inspection tools have been found to be effective tools for process quality control and to increase the yield.

Acknowledgements

This work has been supported by the European Commission as part of Framework 7 ICT 2009 collaborative project HIFLEX (Grant no. 248678).

References

1 C. Candelise, M. Winskel and R. Gross, *Prog. Photovoltaics*, 2012, **20**, 816–831.
2 C. J. M. Emmott, A. Urbina and J. Nelson, *Sol. Energy Mater. Sol. Cells*, 2012, **97**, 14–21.
3 N. Espinosa, R. García-Valverde, A. Urbina and F. C. Krebs, *Sol. Energy Mater. Sol. Cells*, 2011, **95**, 1293–1302.
4 C. European, *Critical raw materials for the EU: report of the ad-hoc working group on defining critical raw materials*, European Commission, 2010.
5 R. L. Moss, E. Tzimas, H. Kara, P. Willis, and J. Kooroshy, *Critical Metals in Strategic Energy Technologies – SETIS*, European Commission, Joint Research Centre, Luxembourg, 2011.
6 B. Zimmermann, M. Glatthaar, M. Niggemann, M. K. Riede, A. Hinsch and A. Gombert, *Sol. Energy Mater. Sol. Cells*, 2007, **91**, 374–378.
7 J. Ajuria, I. Etxebarria, W. Cambarau, U. Muñecas, R. Tena-Zaera, J. C. Jimeno and R. Pacios, *Energy Environ. Sci.*, 2011, **4**, 453.

8 M. Manceau, D. Angmo, M. Jørgensen and F. C. Krebs, *Org. Electron.*, 2011, **12**, 566–574.
9 Y. Galagan, J.-E. J. M. Rubingh, R. Andriessen, C.-C. Fan, P. W. M. Blom, S. C. Veenstra and J. M. Kroon, *Sol. Energy Mater. Sol. Cells*, 2011, **95**, 1339–1343.
10 Y. Galagan, D. J. D. Moet, D. C. Hermes, P. W. M. Blom and R. Andriessen, *Org. Electron.*, 2012, **13**, 3310–3314.
11 Y. Galagan, B. Zimmermann, E. W. C. Coenen, M. Jørgensen, D. M. Tanenbaum, F. C. Krebs, H. Gorter, S. Sabik, L. H. Slooff, S. C. Veenstra, J. M. Kroon and R. Andriessen, *Adv. Energy Mater.*, 2012, **2**, 103–110.
12 D. Angmo, M. Hösel and F. C. Krebs, *Sol. Energy Mater. Sol. Cells*, 2012, **107**, 329–336.
13 T.-H. Han, Y. Lee, M.-R. Choi, S.-H. Woo, S.-H. Bae, B. H. Hong, J.-H. Ahn and T.-W. Lee, *Nat. Photonics*, 2012, **6**, 105–110.
14 A. L. Roes, E. A. Alsema, K. Blok and M. K. Patel, *Progr. Photovolt.: Res. Appl.*, 2009, **17**, 372–393.
15 R. García-Valverde, J. A. Cherni and A. Urbina, *Prog. Photovoltaics*, 2010, **18**, 535–558.
16 F. Lenzmann, J. Kroon, R. Andriessen, N. Espinosa, R. Garcia-Valverde and F. Krebs, 26th EU PVSEC Proceedings, 5–9 September 2011, Hamburg, pp. 3835–3839.
17 F. C. Krebs, T. D. Nielsen, J. Fyenbo, M. Wadstrøm and M. S. Pedersen, *Energy Environ. Sci.*, 2010, **3**, 512–525.
18 ISO 14040, *Environmental management – life cycle assessment – principles and framework*, International Organisation for Standardisation (ISO), Geneva, Switzerland, 1997.
19 Swiss Centre for Life Cycle Inventories, http://www.ecoinvent.org/.
20 G. Hammond and C. Jones, *Inventory of Carbon & Energy (ICE) Version 2.1*, Department of Mechanical Engineering, University of Bath, UK, 2011.
21 N. Espinosa, R. García-Valverde, A. Urbina, F. Lenzmann, M. Manceau, D. Angmo and F. C. Krebs, *Sol. Energy Mater. Sol. Cells*, 2012, **97**, 3–13.
22 F. C. Krebs, R. Søndergaard and M. Jørgensen, *Sol. Energy Mater. Sol. Cells*, 2011, **95**, 1348–1353.
23 D. Angmo, T. T. Larsen-Olsen, M. Jørgensen, R. R. Søndergaard and F. C. Krebs, *Adv. Energy Mater.*, 2013, **3**(2), 172–175.
24 B. Azzopardi, J. Mutale, and D. Kirschen, in *Sustainable Energy Technologies*, *ICSET 2008, IEEE International Conference on 2008*, 2008, pp. 589–594.
25 B. Azzopardi and J. Mutale, *Renewable Sustainable Energy Rev.*, 2010, **14**, 1130–1134.
26 Eurostat, Half-yearly electricity and gas prices, http://www.epp.eurostat.ec.europa.ec/statistics_explained/images/6/64/Energy_prices_2011.xls, 2011.
27 Fraunhofer Institute for Solar Energy Systems, *Photovoltaics Report*, Freiburg, 2012.
28 EU Energy Portal, http://www.energy.eu.
29 B. Azzopardi, C. J. M. Emmott, A. Urbina, F. C. Krebs, J. Mutale and J. Nelson, *Energy Environ. Sci.*, 2011, **4**, 3741–3753.